

May the Best Meme Win!: New Exploration of Competitive Epidemic Spreading over Arbitrary Multi-Layer Networks

Faryad Darabi Sahneh^{1,*} and Caterina Scoglio¹

¹*Electrical and Computer Engineering Department, Kansas State University*

This study extends SIS epidemic model for single virus propagation over an arbitrary graph to SI_1SI_2S epidemic model of two exclusive, competing viruses over a two-layer network with generic structure, where network layers represent the distinct transmission routes of the viruses. We find analytical results determining extinction, mutual exclusion, and coexistence of the viruses by introducing concepts of survival threshold and winning threshold. Furthermore, we show possibility of coexistence in SIS-type competitive spreading over multilayer networks. Not only we prove a coexistence region rigorously, we are able to quantitate it via interrelation of central nodes across the network layers. None or small overlapping of central nodes of each layer is the key determinant of coexistence. Specifically, coexistence is impossible if network layers are identical, while it is possible if the network layers have distinct dominant eigenvectors and node degree vectors. We employ a novel multilayer network generation framework to obtain a set of networks from an initial network so that individual layers have identical graph properties while the interrelation of network layers varies. Therefore, any difference in outputs is purely the result of interrelation. For example, we show both analytically and numerically that positive correlation of network layers makes it difficult for a virus to survive while in a network with negatively correlated layers survival is easier while total removal of the other virus is more difficult.

Keywords: Competing epidemic spreading, multilayer networks, mutual exclusion, coexistence, SI_1SI_2S , survival threshold, winning threshold

I. INTRODUCTION

Spreading of multiple viruses within a single population has shown very rich dynamical characteristics [1] and has attracted a substantial attention recently [2–4]. Applications of these type of models are beyond physiological meaning of virus, for ‘virus’ may refer to products [5], memes [6], pathogens [7], etc. Multiple virus propagation is a mathematically challenging problem. This problem becomes particularly much more complicated if the network through which viruses propagate are distinct. Current knowledge of how hybridity of underlying topology influences fate of the pathogens is very little and limited. These systems are usually mathematically intractable, hindering conclusive results on spreading of multiple viruses on multi-layer networks.

Several interaction possibilities among viruses is another source of complexity for this problem. For example, viruses may be reinforcing [8], weakening [9], exclusive [10], or asymmetric [3, 11]. Newman [10] employed bound percolation to study spreading of two SIR viruses in a host population through a single contact network. The paper proved a coexistence threshold above the classical epidemic threshold, indicating possibility of coexistence for SIR model. In that paper, the first virus initially takes over the network, then the second virus spreads through the resulting residual network. Karrer and Newman [1] further extended the work to the more general case where both viruses spread simultaneously. For SIS epidemic spreading, Wang et al. [12] studied competing

viruses according to SIS model and proved (exclusive) competitive SIS viruses cannot coexist in scale-free networks.

Competing spreading over multilayer networks has generated interesting results. This type of models have implications in several applications like product adoption (e.g. Apple vs. Android smart phones), virus-antidote propagation, meme propagation, opposing opinions propagation, and etc. In competitive spreading scenario, if infected by one virus, a node (individual) cannot be infected by the other virus. Funk and Jansen [2] extended the bond percolation analysis of two competing viruses to the case of a two-layer network, investigating effect of layer overlapping. Granell et al. [9] studied the interplay between spreading of disease and information in a two-layer network consisting of a physical contact network spreading the disease and a virtual overlay network propagating information to stop the disease. They found a meta-critical point for the epidemic onset leading to disease suppression. Importantly, this critical point depends on the awareness dynamics and the overlay network structure. Wei et al. [13] studied SIS spreading of two competitive viruses on an arbitrary two-layer network, deriving sufficient conditions for exponential die-out of each viruses. Following up the work, they introduced a statistical tool, EigenPredict, to predict viral dominance of one competitive virus over the other [4].

In this paper, we address the problem of two competitive viruses propagating in a host population where each virus has distinct contact network for propagation. In particular, we study an SI_1SI_2S model as the simplest extension from SIS model for single virus propagation to competitive spreading of two viruses on a two-layer network. From topology point of view, our study is com-

*Electronic address: faryad@ksu.edu

prehensive because our multilayer network is allowed to have any arbitrary structure.

This paper is most relevant to [13] and [4]. Wei et al. conjectured in [13] and observed in [4] that “*the meme whose first eigenvalue¹ is larger tends to prevail eventually in the composite networks.*” We challenge this argument from two aspects: First, the definition of viral dominance in [4] is related to comparison of fractions of nodes infected by each virus. However, when comparing two viruses with two different contact networks, having a larger eigenvalue is not a direct indicator of a higher final fraction of infected nodes. In fact, it is possible to create two distinct network layers where a meme spreading in the population with smaller eigenvalue takes over a much larger fraction of the population. We find the definition of viral dominance presented in [4] cannot be corroborated with eigenvalues without severe restriction of specific family of networks.

Second, and of paramount interest in this paper, first eigenvalue is a graph property of the layers in isolation and thus does not have the capacity to discuss the joint influence of the network topology, unless some sort of symmetry or homogeneity is assumed. In fact, the generation of one layer of their synthetic multi-layer network via the Erdos Reyni model [4] dictated a homogeneity in their multilayer networks, creating a biased platform for further observations on layer interrelations. Our work more accurately addresses interrelation of networks than presented by Wei et al. [4] because we expanded our exploration beyond viral aggressivity in isolation, that is, we derived formulae to better describe the role of network layers individually as well as their interrelatedness.

We quantitate interrelations of contact layers in terms of spectral properties of a set of matrices. Therefore, our results are not limited to any homogeneity assumption or degree distribution and network model arguments. We find analytical results determining extinction, mutual exclusion, and coexistence of the viruses by introducing concepts of survival threshold and winning threshold. Furthermore, we show possibility of coexistence in SIS-type competitive spreading over multilayer networks. Not only we prove a coexistence region rigorously, we are able to quantitate it via interrelation of central nodes across the network layers. None or small overlapping of central nodes of each layer is the key determinant of coexistence. We employ a novel multilayer network generation framework to obtain a set of networks from an initial network so that individual layers have identical graph properties while the interrelation of network layers varies. Therefore, any difference in outputs is purely the result of interrelation. This makes ours a paradigmatic contribution to shed light on topology hybridity in

multilayer networks.

II. COMPETING EPIDEMICS IN MULTI-LAYER NETWORKS

In this paper, we study a continuous time SI_1SI_2S model of two competing viruses propagating on a two-layer network, initially proposed in [13] in discrete time².

A. Multilayer Network Topology

Consider a population of size N among which two viruses propagate acquiring distinct transmission routes. When represented mathematically, the network topology is essentially a multi-layer network because link types are not identical; one type only allows transmission of virus 1 and the other type only allows transmission of virus 2. Such a multilayer network is represented by $\mathcal{G}(V, E_A, E_B)$, where V is the set of vertices (nodes) and E_A and E_B are set of edges (links). By labeling vertices from 1 to N , adjacency matrices $A \triangleq [a_{ij}]_{N \times N}$ and $B \triangleq [b_{ij}]_{N \times N}$ correspond to edge sets E_A and E_B , respectively, where $a_{ij} = 1$ if node j can transmit virus 1 to node i , otherwise $a_{ij} = 0$, and similarly $b_{ij} = 1$ if node j can transmit virus 2 to node i , otherwise $b_{ij} = 0$. We assume the network layers are symmetric, i.e., $a_{ij} = a_{ji}$ and $b_{ij} = b_{ji}$. Corresponding to adjacency matrices A , we define \mathbf{d}_A as the node degree vector, i.e., $d_{A,i} = \sum_{j=1}^N a_{ij}$, $\lambda_1(A)$ as the largest eigenvalue (or spectral radius) of A , and \mathbf{v}_A as the normalized dominant eigenvector, i.e., $A\mathbf{v}_A = \lambda_1(A)\mathbf{v}_A$ and $\mathbf{v}_A^T \mathbf{v}_A = 1$. For adjacency matrix B , \mathbf{d}_B , $\lambda_1(B)$, and \mathbf{v}_B are defined similarly.

Unlike simple (single-layer) graphs, multilayer networks have not been studied much in network science. We define simple graphs $G_A(V, E_A)$ and $G_B(V, E_B)$ to refer to each isolated layer of the multilayer network $\mathcal{G}(V, E_A, E_B)$. This allows us to argue multilayer network \mathcal{G} in terms of simple graphs G_A and G_B properties and their *interrelation*. FIG. 1 shows a schematics of the two-layer network.

B. SI_1SI_2S Model

The competitive epidemic spreading model in this paper, SI_1SI_2S , is an extension of continuous-time SIS spreading of a single virus on a simple graph (see, [14, 15]) to case of competitive viruses on a two-layer network. In this model, each node is either ‘*Susceptible*,’ ‘ I_1 –*Infected*’ (i.e., infected by virus 1), or ‘ I_2 –*Infected*’ (i.e., infected

¹ Wei et al. [4] defined first eigenvalue of a meme as $\beta\lambda_1 - \delta$, where β is infection probability, δ is curing probability, and λ_1 is spectral radius of the underlying graph layer.

² Wei et al. [13] referred to their model as SI_1I_2S . We prefer SI_1SI_2S as a better candidate to emphasize impossibility of direct transition between I_1 and I_2 in this model.

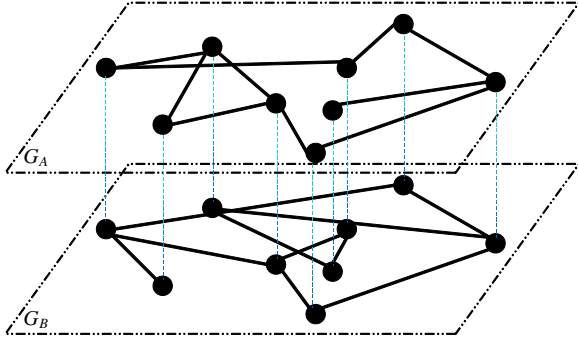


FIG. 1: Schematics of the two-layer contact topology $\mathcal{G}(V, E_A, E_B)$, where a group of nodes share two distinct interactions. In our SI_1SI_2S model, virus 1 transmits exclusively via links of G_A while virus 2 transmits only through links of G_B . Dotted vertical lines emphasize that individual nodes are the same across layers of \mathcal{G} .

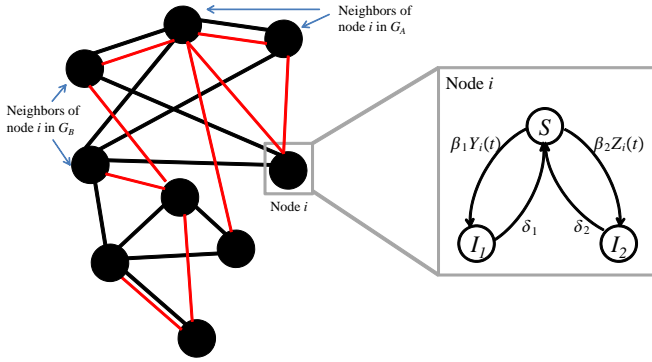


FIG. 2: Schematics of a contact network with the node-level stochastic transition diagram for node i , according to the SI_1SI_2S epidemic spreading model. The parameters β_1 and δ_1 denote virus 1 infection rate and curing rate, respectively, and $Y_i(t)$ is the number of the neighbors of node i in contact graph G_A that are infected by virus 1 at time t . Similarly, β_2 and δ_2 denote virus 2 infection rate and curing rate, respectively, and $Z_i(t)$ is the number of neighbors of node i in contact graph G_B infected by virus 2 at time t .

by virus 2), while virus 1 spreads through E_A edges and virus 2 spreads through E_B edges.

Importantly, in this competitive scenario, the two viruses are exclusive, i.e., *a node cannot be infected by virus 1 and virus 2 simultaneously*.

Consistent with SIS propagation on a single graph ([14, 15]), the infection and curing processes for virus 1 and 2 are characterized by (β_1, δ_1) and (β_2, δ_2) , respectively. To illustrate, the curing process for I_1 -infected node i is a Poisson process with curing rate $\delta_1 > 0$. The infection process for susceptible node i effectively occurs at rate $\beta_1 Y_i(t)$, where $Y_i(t)$ is the number of I_1 -infected neighbors of node i at time t in layer G_A . Curing and infection processes for virus 2 are likewise. FIG. 2 depicts a schematic of competing SIS epidemic spreading over a two-layer network.

The competing spreading process is essentially a cou-

pled Markov process which is mathematically intractable due to exponential explosion of its Markov state space size [16]. To overcome this issue, applying closure techniques results in approximate models with much smaller state space size, however followed by cost of exactness. Specifically, a first order mean-field type approximation [16] suggests the following differential equations for the evolution of probabilities of being infected by virus 1 and 2, denoted by $p_{1,i}$ and $p_{2,i}$ for node i , respectively:

$$\dot{p}_{1,i} = \beta_1(1 - p_{1,i} - p_{2,i}) \sum_{j=1}^N a_{ij} p_{1,j} - \delta_1 p_{1,i}, \quad (1)$$

$$\dot{p}_{2,i} = \beta_2(1 - p_{1,i} - p_{2,i}) \sum_{j=1}^N b_{ij} p_{2,j} - \delta_2 p_{2,i}, \quad (2)$$

for $i \in \{1, \dots, N\}$, which has the state-space size of $2N$. This model is an extension of NIMFA model [14] for SIS spreading on simple graphs.

Competing virus propagation model (1-2) exhibits rich dynamical behavior dependent on epidemic parameters and contact network multi-layer structure. In SIS-type epidemic models, a key characteristic of a virus is its *effective infection rate*, defined as the ratio of the infection rate over the curing rate, measuring the number of attempts of an infected node to infect its neighbors before recovering. Accordingly, depending on values of effective infection rates $\tau_1 \triangleq \frac{\beta_1}{\delta_1}$ and $\tau_2 \triangleq \frac{\beta_2}{\delta_2}$ of virus 1 and 2, several outcomes are possible for SI_1SI_2S model (1-2). In particular, both viruses may extinct ultimately, or one removes the other one, or both coexist.

C. Problem Statement

Linearization of our SI_1SI_2S model (1-2) at the healthy equilibrium (i.e. $p_{1,i} = p_{2,i} = 0, i \in \{1, \dots, N\}$) demonstrates the exponential extinction condition for both viruses: when $\tau_1 < 1/\lambda_1(A)$ and $\tau_2 < 1/\lambda_1(B)$, any initial infections exponentially die out. In this paper, we refer to such critical value as *no-spreading threshold* because for effective infection rates below it the virus is so weak that it cannot spread in the population regardless of any competition with the other virus.

Wei et al. [13] detailed the no-spreading condition as the following: If $\tau_1 < 1/\lambda_1(A)$, virus 1 does not spread and dies out exponentially, and furthermore, exponential extinction of both viruses only occurs if $\tau_1 < 1/\lambda_1(A)$ and $\tau_2 < 1/\lambda_1(B)$ simultaneously. The no-spreading thresholds $\tau_1^0 = 1/\lambda_1(A)$ and $\tau_2^0 = 1/\lambda_1(B)$ for virus 1 and virus 2 are constant and only depend on the topology of each layer. They depend neither on the aggressiveness of the other competing virus, nor on the interrelation of the network layers, the two key factors in competitive epidemic spreading. Exponential extinction is the only analytical result in Wei [13]. While these results are interesting in themselves, scenarios where for both viruses $\tau_1 > 1/\lambda_1(A)$ and $\tau_2 > 1/\lambda_1(B)$ are more interesting.

Problem: Suppose the effective infection rates of each virus is larger than their no-spreading threshold, i.e.,

$\tau_1 > 1/\lambda_1(A)$ and $\tau_2 > 1/\lambda_1(B)$:

1. Will both viruses survive (coexistence) or one virus removes the other completely (mutual exclusion)?
2. Which characteristics of multi-layer network structure will allow coexistence or will force extinction?

These questions correspond to the long term behavior of the competitive spreading dynamics. Hence, to address these questions, we perform a steady-state analysis of SI_1SI_2S model. Specifically, using bifurcation techniques, we define two critical values, namely *survival threshold* and *winning threshold*, which determine whether a virus will survive, and if so, whether it can completely remove the other virus. Significantly, we go beyond these threshold conditions and examine interrelation of network layers. Using eigenvalue perturbation, we find the interrelations of dominant eigenvectors and node-degree vectors of network layers are critical determinants of competitive virus ultimate behaviors.

III. MAIN RESULTS

As explained in the problem statement, the objective of this paper is to study long-term behavior of SI_1SI_2S model for competitive viruses. Hence, bifurcation analysis is a helpful mathematical tool to study the steady-state behavior of SI_1SI_2S model. Application of bifurcation analysis to SIS epidemic model of a single virus on a simple graph determines the critical value that a non-healthy equilibrium emerges, hence determining a survival threshold for the virus. Interestingly, for SIS model no-spreading threshold and survival threshold coincide. However, we expect that for SI_1SI_2S these two critical values are distinct. The reason is a virus may initially spread in an almost entirely susceptible population but then die out as the consequence of competition with a simultaneous virus having a sufficiently stronger infection rate. In fact, the survival threshold is larger than the no-spreading threshold, monotonically increasing with aggressiveness of the other virus.

A virus with an effective infection rate larger than the survival threshold might even be so aggressive that completely removes the other competitive virus. As a consequence, competitive spreading induces an additional threshold concept, the winning threshold, determining the critical value of effective infection rate that a virus will prevail and will be the sole survived.

Even though the determination of the two thresholds for both viruses involves four quantities, we show that winning thresholds can be deduced from survival thresholds. Hence, we only focus on finding survival thresholds. Furthermore, because of expressions duality, with no loss of generality, we only find survival threshold of virus 1.

Unfortunately, the dependency of survival threshold of one virus on the structure of multilayer network topology as well as the aggressiveness of the other competitive virus is so intertwined and complex that hinders any conclusive understanding of the system by itself. Sig-

nificantly, even though complete analytical solution of survival threshold seems impossible, we are able to characterize possible solutions analytically with explicit expressions. This step is a unique contribution to current understanding of competitive spreading over multi-layer networks with solid and quantitative implications on role of network layer interrelations.

A. Threshold Equations

Bifurcation analysis of SI_1SI_2S model equilibriums finds the survival threshold. Our competing virus propagation model (1-2) yields the equilibriums equations:

$$\frac{p_{1,i}^*}{1 - p_{1,i}^* - p_{2,i}^*} = \tau_1 \sum a_{ij} p_{1,j}^*, \quad (3)$$

$$\frac{p_{2,i}^*}{1 - p_{1,i}^* - p_{2,i}^*} = \tau_2 \sum b_{ij} p_{2,j}^*, \quad (4)$$

for $i \in \{1, \dots, N\}$. The healthy equilibrium (i.e., $p_{1,i}^* = p_{2,i}^* = 0, \forall i$) is always a solution to the above equilibrium equation (3-4). Long term persistence of infection in the population is associated with non-zero solution for the equilibrium equations [14]. We use bifurcation theory to identify critical values for effective infection rates τ_1 and τ_2 such that a second equilibrium, aside from the healthy equilibrium, emerges. Two independent parameters, τ_1 and τ_2 , require the critical value for one virus is a function of the effective infection rate of the other virus. Without loss of generality, we find the critical effective infection rate τ_{1c} as a function of τ_2 , thus determining the survival threshold.

Definition: Given τ_2 , the *survival threshold value* τ_{1c} is the smallest effective infection rate that virus 1 steady state infection probability of each node is positive for $\tau_1 > \tau_{1c}$. For τ_2 in $[0, +\infty)$ as an independent variable, τ_{1c} constitutes a *survival threshold curve*, monotonically increasing function of τ_2 , denoted by $\Phi_1(\tau_2)$.

Above definition for survival threshold value indicates that exactly at the threshold value $p_{1,i}^*|_{\tau_1=\tau_{1c}} = 0$ and $\frac{dp_{1,i}^*}{d\tau_1}|_{\tau_1=\tau_{1c}} > 0$ for all $i \in \{1, \dots, N\}$. Taking the derivative of equilibrium equations (3) with respect to τ_1 , and defining

$$w_i \triangleq \frac{dp_{1,i}^*}{d\tau_1}|_{\tau_1=\tau_{1c}}, \quad y_i \triangleq p_{2,i}^*|_{\tau_1=\tau_{1c}}, \quad (5)$$

we find the survival threshold τ_{1c} is the value for which nontrivial solution exists for $w_i > 0$ in

$$w_i = \tau_{1c}(1 - y_i) \sum a_{ij} w_j, \quad (6)$$

where y_i is the solution of:

$$\frac{y_i}{1 - y_i} = \tau_2 \sum b_{ij} y_j, \quad (7)$$

according to equilibrium equation (4).

Equation (6) is an eigenvalue problem. Among all the possible solutions, only

$$\tau_{1c} = \frac{1}{\lambda_1(\text{diag}\{1-y_i\}A)} \quad (8)$$

is acceptable because according to Perron-Frobenius Theorem only the dominant eigenvector of the matrix $\text{diag}\{1-y_i\}A$ has all positive entries, yielding $w_i = \frac{dp_{1,i}^*}{d\tau_1}|_{\tau_1=\tau_{1c}} > 0$.

The eigenvalue problem (6) gives a mathematical way to find the survival threshold τ_{1c} depending on the value of τ_2 . Unfortunately, this implicit dependence hinders clear understanding of the propagation interplay between virus 1 and virus 2.

Finding y_i for all possible values of τ_2 , and then finding the threshold value τ_{c1} from (8), we obtain survival threshold curve $\Phi_1(\tau_2)$ for virus 1. This curve divides the region of (τ_1, τ_2) into two regions, where virus 1 survives versus where virus 1 is extinct. We can use analogous equations to find survival threshold curve $\Phi_2(\tau_1)$ for virus 2. Given τ_2 , we can find τ_{1c} such that for $\tau_1 > \tau_{1c}$, virus 1 can survive.

We can think of another threshold, winning threshold, such that for $\tau_1 > \tau_1^\dagger$, only virus 1 can survive and virus 2 is completely suppressed. Interestingly, winning threshold of virus 1 is in fact the value of τ_1^\dagger such that the survival threshold of virus 2 is τ_2 for $\tau_1 = \tau_1^\dagger$. Therefore, $\Psi_1(\cdot)$ is the inverse function of $\Phi_2(\cdot)$, i.e.,

$$\Psi_1(\tau_2) = \Phi_2^{-1}(\tau_2). \quad (9)$$

Therefore, finding the survival thresholds of both viruses also yields the winning threshold curves. The two curves $\Phi_1(\tau_2)$ and $\Phi_2(\tau_1)$ divide (τ_1, τ_2) plane in four regions: where both viruses are extinct, where only virus 1 survives, where only virus 2 survives, where both viruses survive and coexist. The coexisting region contains the values of (τ_1, τ_2) between survival threshold curves $\Phi_1(\tau_2)$ and $\Phi_2(\tau_1)$.

B. Characterization of Threshold Curves

Complete analytical solution of survival threshold curves is not feasible. Instead, we quantitate interrelations of contact layers to formulate our analytical assertions. We describe conditions for viral coexistence via attaining explicit analytical quantities that give conditions for mutual exclusion and coexistence of viruses. Our approach to tackle this problem is to find explicit solutions to (6) and (7) for values of τ_2 close to $1/\lambda_1(B)$ and for very large values of τ_2 , and then quantitate the survival epidemic curves using these explicit expressions. The rationale for this approach is that at both extreme values, we know solution to (7), and the survival threshold value τ_{1c} . Therefore, we can employ eigenvalue perturbation techniques to find explicit solutions for τ_2 close to $1/\lambda_1(B)$ and τ_2 very large. Results for τ_2 close to

$1/\lambda_1(B)$ applies to the scenario where competitive viruses are *non-aggressive*, whereas results for τ_2 very large corresponds to *aggressive* competition. Behavior of the competitive spreading process for moderate aggressiveness is hence an interpolation of the extreme scenarios of non-aggressive and aggressive propagation.

First, we perform perturbation analysis to find τ_{c1} for values of τ_2 close to $1/\lambda_1(B)$. We know at $\tau_2 = 1/\lambda_1(B)$, $y_i = 0$ solves (7), thus $\tau_{c1} = 1/\lambda_1(A)$ is the survival threshold according to (7). For values of τ_2 close to $1/\lambda_1(B)$, we use eigenvalue perturbation technique and study sensitivity of threshold equation (6) respective to deviation in τ_2 from $1/\lambda_1(B)$. As detailed in the Appendix, we find

$$\frac{d\tau_{1c}}{d\tau_2}|_{\tau_2=1/\lambda_1(B)} = \frac{\lambda_1(B)}{\lambda_1(A)} \frac{\sum v_{A,i}^2 v_{B,i}}{\sum v_{B,i}^3}, \quad (10)$$

expressing the dependency of virus 1 survival threshold (τ_{1c}) to effective infection rate of virus 2 (τ_2) for values of τ_2 close to $1/\lambda_1(B)$. This expression (10) consists of two components: $\frac{\lambda_1(B)}{\lambda_1(A)}$, which is the spectral radius ratio

of each network layers in isolation, and $\frac{\sum v_{A,i}^2 v_{B,i}}{\sum v_{B,i}^3}$, which determines the influence of interrelations of the two layers. Significantly, if $\sum v_{A,i}^2 v_{B,i}$ is small, expression (10) suggests that virus 1 survival threshold is not influenced by virus 2 infection rate. This has very interesting interpretations: when spectral central nodes of G_A , i.e., those nodes with larger element in dominant eigenvector of G_A , are trivially covered by spectral central nodes of G_B , then virus 1 survival threshold does not increase much by τ_2 . In other words, in this case virus 2 does not compete over accessible resources of virus 1, therefore, virus 1 is not affected much by the copropagation. On the other hand, if spectral central nodes of G_A are covered by spectral central nodes of G_B , then $\sum v_{A,i}^2 v_{B,i}$ is maximal indicating considerable dependency of survival threshold of virus 1 on aggressiveness of the other virus. FIG. 3 (a) depicts survival threshold curves for non-aggressive competitive spreading. From (10), the die-out threshold curve $\Phi_1(\tau_2)$ can be approximated close to $(\tau_2, \tau_1) = (\frac{1}{\lambda_1(B)}, \frac{1}{\lambda_1(A)})$ as

$$\Phi_1(\tau_2) \simeq \frac{1}{\lambda_1(A)} \left\{ 1 + \frac{\sum v_{A,i}^2 v_{B,i}}{\sum v_{B,i}^3} (\lambda_1(B)\tau_2 - 1) \right\}. \quad (11)$$

Similar arguments apply to the case of aggressive competing viruses where τ_1 and τ_2 are relatively large. Studying threshold equations (6)-(7) for $\tau_2^{-1} \rightarrow 0$, we find $\frac{\tau_{1c}}{\tau_2}|_{\tau_2 \rightarrow \infty}$ is the inverse of the spectral radius of $D_B^{-1}A$ (see Appendix for detailed derivation):

$$\frac{\tau_{1c}}{\tau_2}|_{\tau_2 \rightarrow \infty} = \frac{1}{\lambda_1(D_B^{-1}A)} = \frac{1}{\lambda_1(D_B^{-1/2}AD_B^{-1/2})}, \quad (12)$$

expressing the dependency of virus 1 survival threshold (τ_{1c}) to effective infection rate of virus 2 (τ_2) for large values of τ_2 . This expression (12) directly points to the

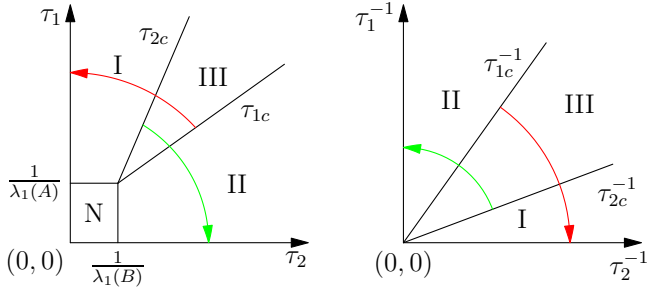


FIG. 3: The survival regions diagrams in SI_1SI_2S model for values of (τ_1, τ_2) close to $(\frac{1}{\lambda_1(A)}, \frac{1}{\lambda_1(B)})$ (left) and for very large values of (τ_1, τ_2) (right). The SI_1SI_2S model with two-layer contact topology exhibits four possibilities: extinction region N where both viruses die-out, mutual extinction region I, where virus 1 survives and virus 2 dies out, mutual extinction region II, where only virus 2 survives and virus 1 dies out, and finally coexistence region III, where both viruses survive and persist in the population. The red arrow shows the survival region of virus 1 (regions I and III) and the green arrow shows the survival region of virus 2 (regions II and III). Note that in (b) very large values of (τ_1, τ_2) are sketched for inverse values thus the origin represents infinitely large values. Equations (10) and (12) analytically find the separating lines between the survival regions in explicit expressions.

influence of interrelations of the two layers. Significantly, if $\lambda_1(D_B^{-1}A)$ is large, expression (10) suggests that virus 1 survival threshold does not increase significantly by virus 2 infection rate. This has very interesting interpretations: when degree central nodes of G_A , i.e., those nodes with larger node degree, are not covered by nodes which also have high degree in G_B , then virus 1 survival threshold does not increase much with τ_2 . In other words, in this case virus 2 cannot compete over major resources of virus 1, therefore, virus 1 is not affected much by the co-propagation. On the other hand, if degree-central nodes of G_A are covered by nodes with high degree in G_B , then $\lambda_1(D_B^{-1}A)$ is small indicating considerable *dependency* of survival threshold of virus 1 on aggressiveness of the other virus. FIG. 3 (b) depicts survival threshold curves for large values of (τ_2, τ_1) by inverting the rates so that point $(0,0)$ belongs to effective infection rates equal to infinity. From (12), the die-out threshold curve $\Phi_1(\tau_2)$ asymptotically becomes

$$\Phi_1(\tau_2) \simeq \frac{1}{\lambda_1(D_B^{-1}A)}\tau_2, \quad (13)$$

for aggressive competitive propagation.

We prove condition for coexistence by showing there is overlapping between regions where viruses survive.

Theorem 1 *In SI_1SI_2S model (1-2) for competing epidemics over multi-layer networks, if the two network layers G_A and G_B are identical, coexistence is impossible, i.e., virus with even a slightly larger effective infection rate dominates and completely removes the other virus. Otherwise, if node-degree vectors of G_A and G_B are not*

parallel, i.e., $\mathbf{d}_A \neq c\mathbf{d}_B$, or dominant eigenvectors of G_A and G_B do not completely overlap, i.e., $\mathbf{v}_A \neq \mathbf{v}_B$ the multi-layer structure of the underlying topology allows a nontrivial coexistence region.

Proof. If $G_A = G_B$, then equation (7) suggests $\tau_{c1} = \tau_2$ solves threshold equation (6). Similarly $\tau_{2c} = \tau_1$, suggesting $\tau_1^\dagger = \tau_2$ according to (9), i.e., survival and winning thresholds coincide. Therefore, the virus with even a slightly larger effective infection rate dominates and completely removes the other virus if the two network layers are identical.

In order to show possibility of coexistence for non-aggressive competitive viruses, we show the survival regions overlap by proving

$$\left. \frac{d\tau_{1,c}}{d\tau_2} \cdot \frac{d\tau_{2,c}}{d\tau_1} \right|_{(\tau_1, \tau_2) = (\frac{1}{\lambda_1(A)}, \frac{1}{\lambda_1(B)})} < 1. \quad (14)$$

Using expression (10) and its counterpart for $\frac{d\tau_{2,c}}{d\tau_1}$, as detailed in Appendix, we find that condition (14) is always true except for the special case where dominant eigenvectors of G_A and G_B completely overlap, i.e., $\mathbf{v}_A = \mathbf{v}_B$.

In order to show possibility of coexistence for aggressive competitive viruses, we show the survival regions overlap by proving

$$\left. \frac{\tau_{1c}}{\tau_2} \right|_{\tau_2 \rightarrow \infty} \times \left. \frac{\tau_{2c}}{\tau_1} \right|_{\tau_2 \rightarrow \infty} < 1. \quad (15)$$

Using expression (12) and its counterpart for $\frac{\tau_{2c}}{\tau_1}|_{\tau_2 \rightarrow \infty}$, as detailed in Appendix section, we find that condition (15) is always true except for the special case where node-degree vectors of G_A and G_B are parallel, i.e., $\mathbf{d}_A = c\mathbf{d}_B$. ■

When dominant eigenvectors of G_A and G_B are not identical, then condition (14) indicates that non-aggressive viruses can coexists. When propagation of competitive viruses is aggressive, condition (15) indicates that viruses can coexists if node-degree vectors of G_A and G_B are not parallel. However, the rare situation where G_A and G_B are not identical, however $\mathbf{d}_A = c\mathbf{d}_B$ and $\mathbf{v}_A = \mathbf{v}_B$, simultaneously, demands further explorations.

The above theorem and equations (10) and (12) signifies the importance of interrelation of network layers. As will be discussed in simulation section, one approach to capture only the effect of interrelation is to generate multilayer networks from two graphs G_A and G_B just by relabeling vertices of G_B . In this way, we will have a set of multilayer networks whose layer graphs are identical but how nodes in one layer corresponds to the nodes of the other varies.

In the context of competitive spreading, whether it being memes, opinions, or product, the population under study serves as the ‘resource’ for the competing entities, thus relating nicely to ‘competing species’ in ecology. Competing species has been long studied in ecology, centering at ‘competition exclusion principle’: *Two species competing for the same resources cannot coexist indefinitely under identical ecological factors. The species with*

the slightest advantage or edge over another will dominate eventually. Our SI_1SI_2S model also predicts when the two network layers are identical, coexistence is not possible. Significantly, different propagation routes break this ‘ecological symmetry,’ allowing coexistence. Not only we proved coexistence region rigorously, we were able to quantitate this ecological asymmetry via interrelation of central nodes across the network layers. None or small overlapping of central nodes of each layer is the key determinant of coexistence. This conclusion is significant because it nicely relates to ‘niche differentiation’ in ecology, and yet is built upon network science rigor.

C. Standardized Threshold Diagram and a Global Approximate Formula

Exploring efficient characterization of threshold curves using extreme scenarios, we propose a standardized threshold diagram, where threshold curves are plotted in a $[0, 1] \times [0, 1]$ plane for $(x, y) = (\frac{1}{\lambda_1(B)\tau_2}, \frac{1}{\lambda_1(A)\tau_1})$, axes scaled by layer spectral radius and inverted. Curves in standardized threshold diagram start from origin to point $(1, 1)$. From (10) and (12) the slopes of the survival curve of virus 1 at $(0, 0)$ and $(1, 1)$ are

$$m_0 = \frac{\lambda_1(B)}{\lambda_1(A)} \lambda_1(D_B^{-1}A), \quad (16)$$

$$m_1 = \frac{\sum v_{A,i}^2 v_{B,i}}{\sum v_{B,i}^3}, \quad (17)$$

respectively. Importantly, these slopes bring into being a parametric approximation for survival threshold curve $\tau_{1c} = \Phi_1(\tau_2)$ for the full range of τ_2 . We use a quadratic Bezier curve:

$$\begin{bmatrix} x \\ y \end{bmatrix} = 2\sigma(1 - \sigma) \begin{bmatrix} a \\ b \end{bmatrix} + \sigma^2 \begin{bmatrix} 1 \\ 1 \end{bmatrix}, \quad (18)$$

connecting $(x, y) = (0, 0)$ to $(x, y) = (1, 1)$ for $\sigma \in [0, 1]$, satisfying the slope constraints (16) and (17), if a and b are chosen as:

$$a = \frac{1 - m_1}{m_0 - m_1}, b = \frac{m_0(1 - m_1)}{m_0 - m_1}. \quad (19)$$

Therefore, Bezier curve (18) approximates the standardized threshold curve diagram for the whole range of $\tau_1 > 1/\lambda_1(A)$ and $\tau_2 > 1/\lambda_1(B)$ using only spectral information of a set of matrices.

D. Multi-layer Network Metric for Competitive Spreading

Proving coexistence is one of the significant contributions of this paper. We can move further and define a

topological index $\Gamma_s(\mathcal{G})$ to quantify coexistence possibility in a multi-layer network $\mathcal{G} = (V, E_A, E_B)$ as

$$\Gamma_s(\mathcal{G}) = 1 - \frac{(\sum v_{B,i} v_{A,i}^2)(\sum v_{A,i} v_{B,i}^2)}{(\sum v_{B,i}^3)(\sum v_{A,i}^3)}.$$

Values of $\Gamma_s(\mathcal{G})$ varies from 0, corresponding to the case where $\mathbf{v}_A = \mathbf{v}_B$, to 1. Values of $\Gamma_s(\mathcal{G})$ close to zero implies coexistence is rare and any survived virus is indeed the absolute winner. $\Gamma_s(\mathcal{G})$ closer to 1 indicates coexistence is very possible on \mathcal{G} . Therefore, $\Gamma_s(\mathcal{G})$ can be used to discuss coexistence for non-aggressive competing viruses.

Similar to the case of non-aggressive competitive spreading, we can define a topological index $\Gamma_l(\mathcal{G})$ to quantify coexistence possibility in a multi-layer network $\mathcal{G} = (V, E_A, E_B)$ as

$$\Gamma_l(\mathcal{G}) = 1 - \frac{1}{\lambda_1(D_B^{-1}A)} \cdot \frac{1}{\lambda_1(D_A^{-1}B)}.$$

Values of $\Gamma_l(\mathcal{G})$ varies from 0, corresponding to the case where $\mathbf{d}_A = \mathbf{c}\mathbf{d}_B$, to 1. Values of $\Gamma_l(\mathcal{G})$ close to zero implies coexistence is rare and any survived virus is indeed the absolute winner. $\Gamma_l(\mathcal{G})$ closer to 1 indicates coexistence is very possible on \mathcal{G} . Therefore, $\Gamma_l(\mathcal{G})$ can be used to discuss coexistence for aggressive competitive viruses.

E. Numerical Simulations

Multi-layer network generation: Our objective is not only to test our analytical formulae, but also to investigate our prediction of cross-layer interrelation effect on competing epidemics. This objective demands a set of two-layer networks that have exactly same layer graphs in isolation, but how these layers are interrelated is varied, hence capturing the *pure effect of interrelation*. Specifically in the following numerical simulations, the contact network G_A through which virus 1 propagates is a random geometric graph with $N = 1000$ nodes, where pairs less than $r_c = \sqrt{\frac{2 \log(N)}{\pi N}}$ apart connect to ensure connectivity. For the contact graph of virus 2 (G_B), we first generated a scale-free network according to the Barabási–Albert model. We then used a randomized greedy algorithm to associate the nodes of this graph with the nodes of G_A , approaching a certain degree correlation coefficient ρ with G_A , i.e., each iteration step permutes nodes when the degree correlation coefficient

$$\rho(\mathcal{G}) = \frac{\sum (d_{A,i} - \bar{d}_A)(d_{B,i} - \bar{d}_B)}{\sqrt{\sum (d_{A,i} - \bar{d}_A)^2} \sqrt{\sum (d_{B,i} - \bar{d}_B)^2}},$$

is closer to the desired value. Specifically, we obtained three different permutations where the generated graphs are negatively ($\rho = -0.47$), neutrally ($\rho = 0$), and positively ($\rho = 0.55$) correlated with G_A . These three graphs are *identical in isolation, yet distinct respective to G_A* .

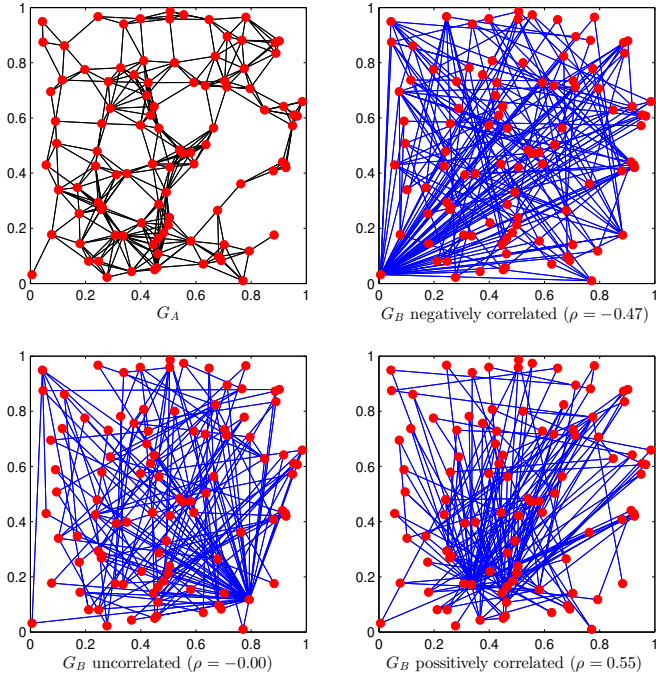


FIG. 4: *Two-layer network generation for numerical simulations is generated here.* The contact network G_A through which virus 1 propagates is a random geometric graph where pairs of nodes with a distance less than $r_c = \sqrt{\frac{2 \log(N)}{\pi N}}$ are connected to each other. For visualization convenience, number of nodes is $N = 100$, which is different from the actual $N = 1000$ used for numerical simulation results. For the contact graph of virus 2 (G_B), we first generated a scale-free network according to the B-A model, associating the nodes of this graph with the nodes of G_A to achieve a certain correlation coefficient with G_A . Specifically, we obtained three different permutations such that the generated graphs are negatively ($\rho = -0.47$), neutrally ($\rho = 0$), and positively ($\rho = 0.55$) correlated with G_A . These three graphs are the same if isolated, and they are distinguished respective to their interrelation with G_A . The high degree nodes in the positively correlated G_B (lower right) have also high degree in G_A (upper left), while the high degree nodes in the negatively correlated G_B (upper right) have low degree size in G_A . The uncorrected G_B (lower left) shows no clear association.

FIG. 4 depicts a graph G_A and three graphs of G_B with $N = 100$ nodes for visualization convenience. The high-degree nodes in the positively correlated G_B (lower right) are also high-degree in G_A (upper left), yet the high-degree nodes in the negatively correlated G_B (upper right) show low degree size in G_A . The uncorrected G_B (lower left) shows no clear association.

Steady-state infection fraction: When the spreading of a single virus is modeled as SIS, the steady-state infection fraction $\bar{p}^{ss} = \frac{1}{N} \sum p_i$ illustrates a threshold phenomena respective to effective infection rates: steady-state infection fraction \bar{p}^{ss} is zero for effective infection rates less than a critical value but becomes positive for larger values. When two viruses compete to spread,

steady state fraction of infection $\bar{p}_1^{ss} = \frac{1}{N} \sum p_{1,i}$ of virus 1 in the SI model exhibits a threshold behavior at $\tau_1 = \tau_{1c}$, for a given τ_2 . FIG. 5 depicts the steady state infection fraction of virus 1 in the SI_1SI_2S competing spreading model (red curve) as a function of effective infection rate τ_1 . In this simulation, effective infection rate of virus 2 is fixed at $\tau_2 = 4 \cdot \frac{1}{\lambda_1(B)}$ and G_B is positively correlated with G_A ($\rho = 0.55$). In order to obtained a unified form, we normalized the vertical axis to $\tau_1 \lambda_1(A)$. The steady state infection fraction of virus 1, \bar{p}_1^{ss} , is zero for $\tau_1 \leq \tau_{1c} \simeq 2.4 \frac{1}{\lambda_1(A)}$, identifying this range as an extinction region for virus 1; while \bar{p}_1^{ss} is positive for $\tau_1 > \tau_{1c}$ indicating survival of virus 1. Interestingly, aside from the survival threshold τ_{1c} , the winning threshold τ_1^* appears in the figure when plotted against a single virus case: \bar{p}_1^{ss} is assigned the same value as the single virus case for effective infection rates larger than the winning threshold τ_1^\dagger . For example FIG. 5 shows, \bar{p}_1^{ss} in the competing scenario (red curve) is exactly similar to the case of single virus propagation (black curve) for $\tau_1 > \tau_1^\dagger \simeq 4.4 \frac{1}{\lambda_1(A)}$. Hence, this region is identified as the absolute winning range for virus 1. For $\tau_1 \in (\tau_{1c}, \tau_1^\dagger)$, virus 1 and virus 2 each persist in the population, marking this range as the coexistence region.

FIG. 6 explores the dependency of steady-state infection fraction curve on network layer interrelation. When contact network of virus 2 (G_B) is positively correlated with that of virus 1 (G_A) it is more difficult for virus 1 to survive, making the survival threshold τ_{1c} relatively larger for positively correlated G_B . Negatively correlated contact network layers impede virus 1 from completely suppress virus 2, making winning threshold τ_1^\dagger larger for negatively correlated G_B .

Survival diagram: Allowing variation of τ_2 , the steady-state infection curve extends to the steady-state infection surface. FIG. 7 plots steady-state fraction of infection for virus 1 (a) and virus 2 (b) as a function of τ_1 and τ_2 . White curves represent theoretical threshold curves derived from the solution to (6), accurately separating the survival regions.

FIG. 8 plots standardized threshold diagram for case where G_B is negatively correlated with G_A (left) and the case where G_B is positively correlated with G_A (right). Predictions from analytical approximation formula (18) turn out to fairly accurately find the threshold curves. Our standardized threshold diagram shows three survival regions: mutual extinction region I, where only virus 1 survives and virus 2 dies out, mutual extinction region II, where only virus 2 survives and virus 1 dies out, and finally coexistence region III, where both viruses survive and persist in the population.

IV. DISCUSSION AND CONCLUSION

Our model for competing multi-virus propagation shows very rich dynamics, beyond those of single virus

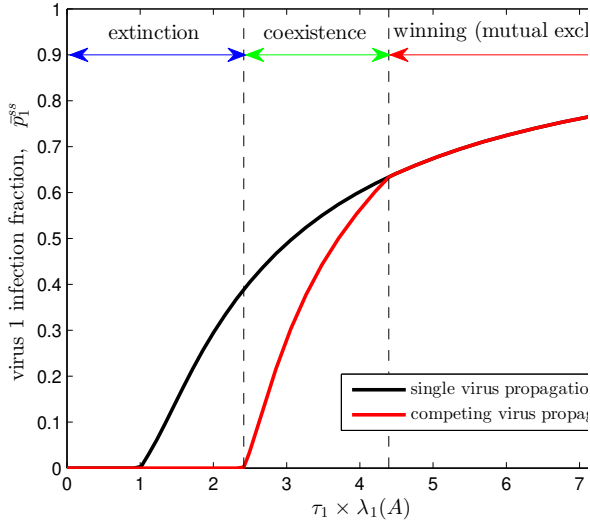


FIG. 5: *Steady state infection fraction of virus 1 in SI_1SI_2S competing spreading model (red curve) as a function of effective infection rate τ_1 . The black curve represents the steady state fraction according to single virus SIS model. In this simulation, the effective infection rate of virus 2 is fixed at $\tau_2 = 4 \cdot \frac{1}{\lambda_1(B)}$ and G_B is positively correlated with G_A ($\rho = 0.55$). Choosing $\tau_1 \lambda_1(A)$ as the independent variable normalizes the vertical axis. The steady-state infection fraction of virus 1 (\bar{p}_1^{ss}) is zero for $\tau_1 \leq \tau_{1c} \simeq 2.4 \frac{1}{\lambda_1(A)}$, an extinction region for virus 1. Interestingly, for $\tau_1 > \tau_1^* \simeq 4.4 \frac{1}{\lambda_1(A)}$, \bar{p}_1^{ss} for the competing scenario (red curve) is exactly similar to the case of single virus propagation (black curve), suggesting extinction of virus 2, hence marking this region as the winning range for virus 1. For $\tau_1 \in (\tau_{1c}, \tau_1^*)$, virus 1 and virus 2 both persist in the population, making coexistence regions.*

propagation. This type of modeling is propagation of exclusive entities, for ex opinions about a subject, where people or neutral; spreading of a disease through contact and viral propagation of antidote lute immunity to the disease, or marketing of competing products like Android versus Apple smartphone.

Furthermore, it highlights the importance of generic structure of in our model because degree distribution random network models are restricted, producing restricted and biased conclusions. In fact, no restriction on the structure of multi-layer network is a major significance for network layers in realistic social context are highly hybrid and in many cases engineered that classical random network models hardly lead to reliable outcomes.

We believe our methodology has great potentials for application to broader classes of multi-pathogen spreading over multi-layer and interconnected networks. Exploration of SI_1SI_2S transient dynamics model will greatly enhance our understanding of this complex problem, complementing results of this paper on ‘ultimate behaviors’ of this model.

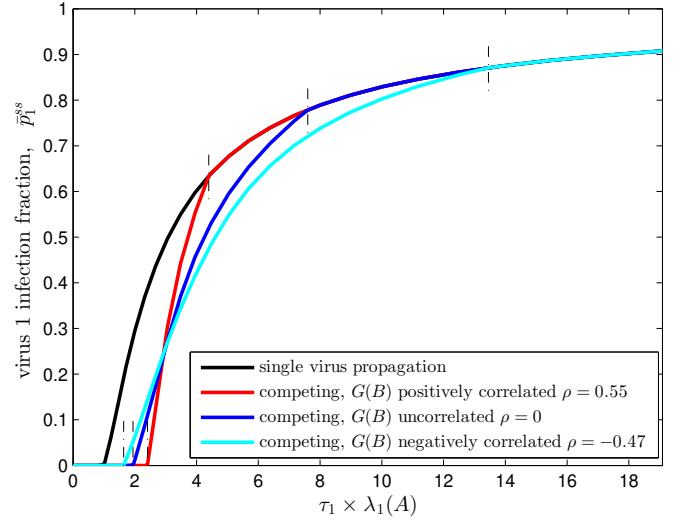


FIG. 6: *Steady-state infection fraction of virus 1 in the SI_1SI_2S competing spreading model (red curve) as a function of effective infection rate τ_1 . The black curve represents the steady-state fraction of SIS model. In this simulation, effective infection rate of virus 2 is fixed at $\tau_2 = 4 \cdot \frac{1}{\lambda_1(B)}$. Point where \bar{p}_1^{ss} becomes non-zero is the survival threshold τ_{1c} , and where \bar{p}_1^{ss} gets the same value as the single virus case (black curve) is the winning threshold τ_1^* . Survival threshold τ_{1c} is larger for positively correlated G_B , indicating it is more difficult to survive positively correlated G_B , while τ_1^* is larger for negatively correlated G_B , indicating it is more difficult to completely suppress the other virus in negatively correlated G_B .*

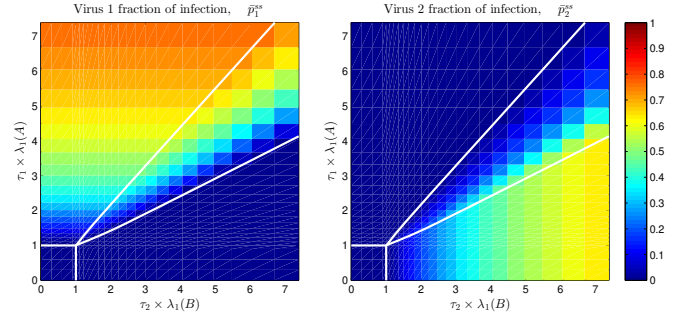


FIG. 7: *Steady state fraction of infection for virus 1 (a) and virus 2 (b) as a function of τ_1 and τ_2 . White curves are theoretical threshold curves accurately separating the survival regions.*

Appendix: Selected Proofs

1. Derivation of Eigenvalue Perturbation Formulae

Here, we detail the derivations of (10) and (12).

At $\tau_2 = 1/\lambda_1(B)$, (7) finds $y_i = 0$ for all nodes. Equation (7) is indeed the steady state equation for infection probabilities in NIMFA model. Van Mieghem [14] found for SIS model the derivative with respect to effective in-

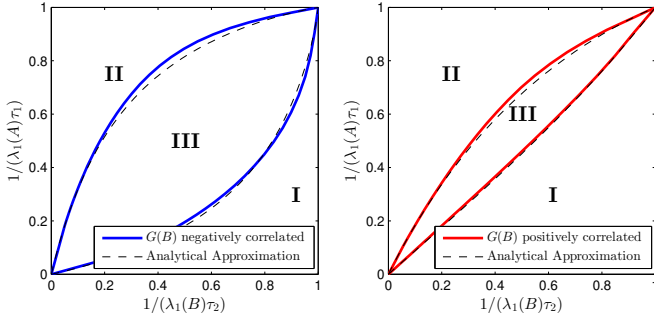


FIG. 8: Standardized threshold diagram for case where G_B is negatively correlated with G_A (left) and the case where G_B is positively correlated with G_A (right). Dashed lines are the predictions from analytical approximation formula explicitly expressed in (18). Standardized threshold diagram shows three survival regions: mutual extinction region I, where only virus 1 survives and virus 2 dies out, mutual extinction region II, where only virus 2 survives and virus 1 dies out, and finally coexistence region III, where both viruses survive and persist in the population.

fection rate, suggesting

$$\frac{dy_i}{d\tau_2}\bigg|_{\tau_2=\frac{1}{\lambda_1(B)}} = c_B v_{B,i}, \quad (\text{A.1})$$

$$w_i\big|_{\tau_2=\frac{1}{\lambda_1(B)}} = c_A v_{A,i} \quad (\text{A.2})$$

where

$$c_A = \frac{\lambda_1(A)}{\sum v_{A,i}^3}, \quad c_B = \frac{\lambda_1(B)}{\sum v_{B,i}^3}, \quad (\text{A.3})$$

where v_A and v_B are the normalized dominant eigenvectors of A and B , respectively.

Differentiating (6) with respect to τ_2 yields:

$$\begin{aligned} \frac{dw_i}{d\tau_2} &= \frac{d\tau_{1c}}{d\tau_2} (1 - y_i) \sum a_{ij} w_j \\ &\quad + \tau_{1c} \left(-\frac{dy_i}{d\tau_2}\right) \sum a_{ij} w_j \\ &\quad + \tau_{1c} (1 - y_i) \sum a_{ij} \frac{dw_j}{d\tau_2}. \end{aligned} \quad (\text{A.4})$$

Inserting $\tau_{1c} = 1/\lambda_1(A)$, $w_i = c_A v_{A,i}$, $y_i = 0$, and $dy_i/d\tau_2 = c_B v_{B,i}$, above equation changes to:

$$\left(I - \frac{1}{\lambda_1(A)} A\right) \frac{d\mathbf{w}}{d\tau_2} = \left(\frac{d\tau_{1c}}{d\tau_2}\right) \lambda_1(A) c_A \mathbf{v}_A - c_B c_A (\mathbf{v}_B \circ \mathbf{v}_A) \quad (\text{A.5})$$

in the collective form, where the Hadamard product \circ acts entry-wise. Multiplying both sides by \mathbf{v}_A^T from left yields

$$\begin{aligned} \frac{d\tau_{1c}}{d\tau_2}\bigg|_{\tau_2=\frac{1}{\lambda_1(B)}} &= \frac{1}{\lambda_1(A)} c_B \mathbf{v}_A^T (\mathbf{v}_B \circ \mathbf{v}_A) \\ &= \frac{\lambda_1(B)}{\lambda_1(A)} \frac{\sum v_{A,i}^2 v_{B,i}}{\sum v_{B,i}^3}, \end{aligned} \quad (\text{A.6})$$

obtaining (10). Finding $\frac{d\tau_{1c}}{d\tau_2}$ at $\tau_2 = 1/\lambda_1(B)$ obtains the dependence of τ_{1c} on τ_2 close to $1/\lambda_1(B)$.

Replacing for $1 - y_i = \frac{\tau_2^{-1}}{\tau_2^{-1} + \sum b_{ij} y_j}$ from (7) into (6) yields

$$w_i = \left(\frac{\tau_{1c}}{\tau_2}\right) \left(\frac{1}{\tau_2^{-1} + \sum b_{ij} y_j}\right) \sum a_{ij} w_j. \quad (\text{A.7})$$

When effective infection rate τ_2 is enormous $\tau_2^{-1} \rightarrow 0$ and $y_i \rightarrow 1$, suggesting

$$w_i = \left(\frac{\tau_{1c}}{\tau_2}\bigg|_{\tau_2 \rightarrow \infty}\right) \frac{1}{d_{B,i}} \sum a_{ij} w_j, \quad (\text{A.8})$$

where $d_{B,i}$ is the B -degree of node i . Therefore, $\frac{\tau_{1c}}{\tau_2}\big|_{\tau_2 \rightarrow \infty}$ is the inverse of the spectral radius of $D_B^{-1}A$, hence proving (12) for large values of τ_2 .

2. Coexistence Proofs

Coexistent region non-aggressive competitive viruses:

To investigate the coexistence region for non-aggressive viruses we shown that (14) is true. From (10), we find

$$\begin{aligned} \frac{d\tau_{1c}}{d\tau_2} \times \frac{d\tau_{2c}}{d\tau_1}\bigg|_{(\tau_1, \tau_2) = (\frac{1}{\lambda_1(A)}, \frac{1}{\lambda_1(B)})} &= \frac{(\sum v_{B,i} v_{A,i}^2)(\sum v_{A,i} v_{B,i}^2)}{(\sum v_{B,i}^3)(\sum v_{A,i}^3)} \end{aligned} \quad (\text{A.9})$$

From Hölder's inequality

$$\begin{aligned} \sum v_{B,i} v_{A,i}^2 &= \sum (v_{B,i}^3)^{1/3} (v_{A,i}^2)^{2/3} \\ &\leq (\sum v_{B,i}^3)^{1/3} (\sum v_{A,i}^3)^{2/3}, \end{aligned} \quad (\text{A.10})$$

and the equality happens iff $\mathbf{v}_A = \mathbf{v}_B$. Similarly,

$$\sum v_{A,i} v_{B,i}^2 \leq (\sum v_{B,i}^3)^{2/3} (\sum v_{A,i}^3)^{1/3} \quad (\text{A.11})$$

Multiplying sides of (A.10) and (A.11) yields

$$(\sum v_{B,i} v_{A,i}^2)(\sum v_{A,i} v_{B,i}^2) \leq (\sum v_{B,i}^3)(\sum v_{A,i}^3), \quad (\text{A.12})$$

proving (A.9) is true.

Coexistent region for aggressive competitive viruses:

To investigate the coexistence region for non-aggressive viruses we shown that (14) is true. Substituting from (12) yields

$$\begin{aligned}
\frac{\tau_{1c}}{\tau_2}|_{\tau_2 \rightarrow \infty} \cdot \frac{\tau_{2c}}{\tau_1}|_{\tau_1 \rightarrow \infty} &= \frac{1}{\lambda_1(D_B^{-1}A)} \cdot \frac{1}{\lambda_1(D_A^{-1}B)} \\
&= \frac{1}{\lambda_1(D_B^{-1}A \otimes D_A^{-1}B)} \\
&= \frac{1}{\lambda_1[(D_B^{-1} \otimes D_A^{-1})(A \otimes B)]} \\
&= \frac{1}{\lambda_1[(D_B \otimes D_A)^{-1}(A \otimes B)]}, \tag{A.13}
\end{aligned}$$

according to properties of Kronecker product.

Degree diagonal matrix of $(A \otimes B)$ is $(D_A \otimes D_B)$. Therefore, $(D_B \otimes D_A)$ is a diagonal permutation of degree diagonal matrix of $(A \otimes B)$. According to Lemma 1, presented in the following, $\lambda_1[(D_B \otimes D_A)^{-1}(A \otimes B)] \geq 1$, thus

$$\frac{\tau_{1c}}{\tau_2}|_{\tau_2 \rightarrow \infty} \cdot \frac{\tau_{2c}}{\tau_1}|_{\tau_1 \rightarrow \infty} \leq 1, \tag{A.14}$$

and equality holds only if $D_B \otimes D_A = D_A \otimes D_B$, which holds only if ratio of B -degree and A -degree of each node is same for all nodes.

Lemma 2 *If $H = \pi(D_C)^{-1}C$, where $\pi(D_C)$ is a diagonal permutation of degree diagonal matrix of symmetric matrix C , then $\lambda_1(H) \geq 1$. Furthermore, equality holds only if $\pi(D_C) = D_C$.*

Proof. Largest eigenvalue maximizes Rayleigh quotient, therefore

$$\begin{aligned}
\lambda_1(H) &= \lambda_1(\pi(D_C)^{-1}C) = \lambda_1(\pi(D_C)^{-1/2}C\pi(D_C)^{-1/2}) \\
&= \max_x \frac{x^T \pi(D_C)^{-1/2}C\pi(D_C)^{-1/2}x}{x^T x} \\
&\geq \frac{1^T C 1}{1^T \pi(D_C) 1} = \frac{\sum d_{C,i}}{\sum d_{C,\pi_i}} = 1,
\end{aligned}$$

where d_{C,π_i} is the degree of node i map. Therefore, $\lambda_1(H) \geq 1$.

Equality holds only if $x = \pi(D_C)^{1/2}1$ is the dominant eigenvector of $\pi(D_C)^{-1/2}C\pi(D_C)^{-1/2}$, i.e., $\pi(D_C)^{-1/2}C1 = \pi(D_C)^{1/2}1$, which only holds if $d_{C,\pi_i} = d_{C,i}$. ■

3. Steady State Numerical Solution

Given $\tau_2 > 1/\lambda_1(B)$, (6) and (7) still numerically find $\tau_{1,c}$. We now define $x_i \triangleq \frac{y_i}{1-y_i}$, given the recursive iteration law:

$$x_i(k+1) = \tau_2 \sum b_{ij} \frac{x_j(k)}{1+x_j(k)} \tag{A.15}$$

to prove to converge exponentially, thus numerically solving (7) as $\frac{x_i(k)}{1+x_i(k)} \rightarrow y_i$. The main advantage of finding equilibrium values using recursive law (A.15) instead of solving ordinary differential equations of the model is that recursive law (A.15) is in discrete steps and unlike ODE's does not require incremental time increase, hence making computations drastically faster.

Furthermore, the steady-state infection probabilities in (3)-(4) can be found via the recursive iteration law:

$$x_i(k+1) = \tau_1 \sum a_{ij} \frac{x_j(k)}{1+x_j(k)+z_j(k)}, \tag{A.16}$$

$$z_i(k+1) = \tau_2 \sum b_{ij} \frac{z_j(k)}{1+x_j(k)+z_j(k)}, \tag{A.17}$$

as $\frac{x_i(k)}{1+x_i(k)+z_i(k)} \rightarrow p_{1,i}^*$ and $\frac{z_i(k)}{1+x_i(k)+z_i(k)} \rightarrow p_{2,i}^*$.

-
- [1] B. Karrer and M. Newman, *Physical Review E*, **84**(3), 036106 (2011). Competing epidemics on complex networks.
 - [2] S. Funk and V. A. Jansen, *Physical Review E*, **81**(3), 036118 (2010). Interacting epidemics on overlay networks.
 - [3] Y.-Y. Ahn, H. Jeong, N. Masuda, and J. D. Noh, *Physical Review E*, **74**(6), 066113 (2006). Epidemic dynamics of two species of interacting particles on scale-free networks.
 - [4] X. Wei, N. C. Valler, B. A. Prakash, I. Neamtui, M. Faloutsos, and C. Faloutsos, *Selected Areas in Communications, IEEE Journal on*, **31**(6), 1049–1060 (2013). Competing memes propagation on networks: A network science perspective.
 - [5] S. Aral and D. Walker, *Management Science*, **57**(9), 1623–1639 (2011). Creating social contagion through viral product design: A randomized trial of peer influence in networks.
 - [6] L. Weng, A. Flammini, A. Vespignani, and F. Menczer, *Scientific Reports*, **2** (2012). Competition among memes in a world with limited attention.
 - [7] S. Shrestha, A. A. King, and P. Rohani, *PLoS computational biology*, **7**(8), e1002135 (2011). Statistical inference for multi-pathogen systems.
 - [8] M. Newman and C. Ferrario, *arXiv preprint arXiv:1305.4648* (2013). Interacting epidemics and coinfection on contact networks.
 - [9] C. Granell, S. Gomez, and A. Arenas, *arXiv preprint arXiv:1306.4136* (2013). On the dynamical interplay between awareness and epidemic spreading in multiplex networks.
 - [10] M. E. Newman, *Physical review letters*, **95**(10), 108701 (2005). Threshold effects for two pathogens spreading on a network.

- [11] Q. Wu, M. Small, and H. Liu, *Journal of Nonlinear Science*, **23**(1), 113–127 (2013). Superinfection behaviors on scale-free networks with competing strains.
- [12] Y. Wang, G. Xiao, and J. Liu, *New Journal of Physics*, **14**(1), 013015 (2012). Dynamics of competing ideas in complex social systems.
- [13] X. Wei, N. Valler, B. A. Prakash, I. Neamtiu, M. Faloutsos, and C. Faloutsos, *ACM SIGCOMM Computer Communication Review*, **42**(5), 5–12 (2012). Competing memes propagation on networks: a case study of composite networks.
- [14] P. Van Mieghem, J. Omic, and R. Kooij, *IEEE/ACM Transactions on Networking*, **17**(1), 1–14 (2009). Virus spread in networks.
- [15] A. Ganesh, L. Massoulie, and D. Towsley in *Proceedings IEEE INFOCOM*, Vol. 2, pages 1455–1466, 2005.
- [16] F. D. Sahneh, C. Scoglio, and P. Van Mieghem, *IEEE/ACM Transaction on Networks*, to appear (2013). Generalized epidemic mean-field model for spreading processes over multi-layer complex networks.

